
Biomechanics of the giant reed *Arundo donax*

H.-Ch. Spatz, H. Beismann, F. Brüchert, A. Emanns and Th. Speck

Phil. Trans. R. Soc. Lond. B 1997 **352**, 1-10

doi: 10.1098/rstb.1997.0001

Email alerting service

Receive free email alerts when new articles cite this article - sign up in the box at the top right-hand corner of the article or click [here](#)

To subscribe to *Phil. Trans. R. Soc. Lond. B* go to: <http://rstb.royalsocietypublishing.org/subscriptions>

Biomechanics of the giant reed *Arundo donax*

H.-CH. SPATZ¹, H. BEISMANN², F. BRÜCHERT², A. EMANNS¹
AND TH. SPECK²

¹ *Institute for Biology III, Schänzlestr. 1, D-79104 Freiburg i.Br., Germany*

² *Botanical Garden, Schänzlestr. 1, D-79104 Freiburg i.Br., Germany*

SUMMARY

The quantitative description of local buckling of hollow plant stems requires the knowledge of Young's modulus in the longitudinal and tangential directions for the different tissues of which the stem is composed. For thick-walled stems the shear modulus for the radial–tangential plane is needed for an advanced treatment of the process of ovalization. The primary causes of failure can be predicted if critical compressive strains in the longitudinal direction and critical tensile strains in the tangential direction are known. All of these mechanical properties and their variation along the length of the stem can be measured in *Arundo donax*.

1. INTRODUCTION

Arundo donax is a giant reed with a hollow stem, perennial in the Mediterranean. With an outer diameter of approximately 2–3 cm it grows to a height of 4–6 m. The stem is reinforced by nodes at distances of roughly 20 cm, less in the lowermost and in the uppermost parts of the plant (figure 1*a*). Cross-sections reveal a structure consisting of a thin outer hypodermal sterome with sclerenchymatous fibres and a much thicker parenchymatous inner ring containing many vascular bundles (figure 1*b*). These have heavily lignified bundle sheaths, giving the structure reinforcement in the longitudinal direction.

Upon bending under wind loads the stems are endangered by local buckling initiated by failure of the material under compressive strains, or by longitudinal splitting due to ovalization of the cross-section (Spatz & Speck 1994). Since analytical solutions (von Kármán 1911; Brazier 1927) for anisotropic and inhomogeneous materials do not exist and even finite element analysis proves to be very difficult and time consuming (Mattheck 1992; Kesel & Labisch 1996), we have developed a numerical treatment of local buckling. The process of ovalization is treated as an equilibrium between the energy necessary to deform a circular cross-section and the energy gained by relaxation of strains in the longitudinal direction (Spatz *et al.* 1990, 1993). The theory was extended to incorporate the stabilizing influence of nodal thickenings (Spatz & Speck 1994). Recently we developed a better description of the deformation of thick-walled circular rings by taking into account the local equilibrium between bending and shear deformations (Spatz *et al.* 1995). The mechanical properties that have to be known for the theoretical description are the Young's moduli in the longitudinal and tangential directions for the different tissues, the shear modulus for the radial–tangential plane and the critical strains in the longitudinal and tangential directions.

This article describes how these data were obtained and how they vary with the height of the stem above ground. The calculation of the maximal bending moments, based on these data, are compared with direct determinations and with bending moments generated by wind loads on the stem.

(a) Terminology

Even on a macroscopic level structures of biological origin are almost never homogeneous. To cope with the difficulty Rowe & Speck (1996) introduced the term 'structural Young's modulus' to describe the stiffness of a structure as a whole. The structural Young's modulus depends on the properties of the tissues comprising a structure but also on their distribution. It will therefore also depend on the particular type of mechanical loading applied. Here we use the term Young's modulus to describe the property of a single homogeneous (not necessarily isotropic) material. If a structure is built from two or more materials with different mechanical properties, we use the term 'structural Young's modulus'. Curvature as used here is the inverse of the radius of curvature at the vertex (cf. figure 2) and has the dimension m^{-1} . The critical curvature is defined as the curvature at the point of final failure of the structure.

The terms longitudinal, tangential and radial are used with respect to the plant stem.

2. MATERIAL AND METHODS

(a) Material

Arundo donax was obtained from the Botanical Garden in Freiburg, Germany, and natural habitats near Montpellier, France. For all mechanical tests the leaf sheaths were removed.

(b) Stem anatomy

The parameters describing the distribution of tissues in a cross-section are described by Spatz *et al.* (1993).

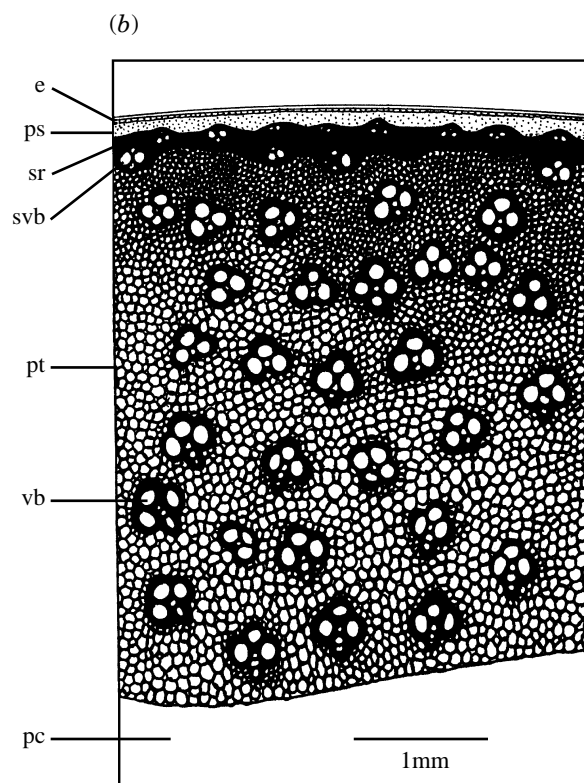
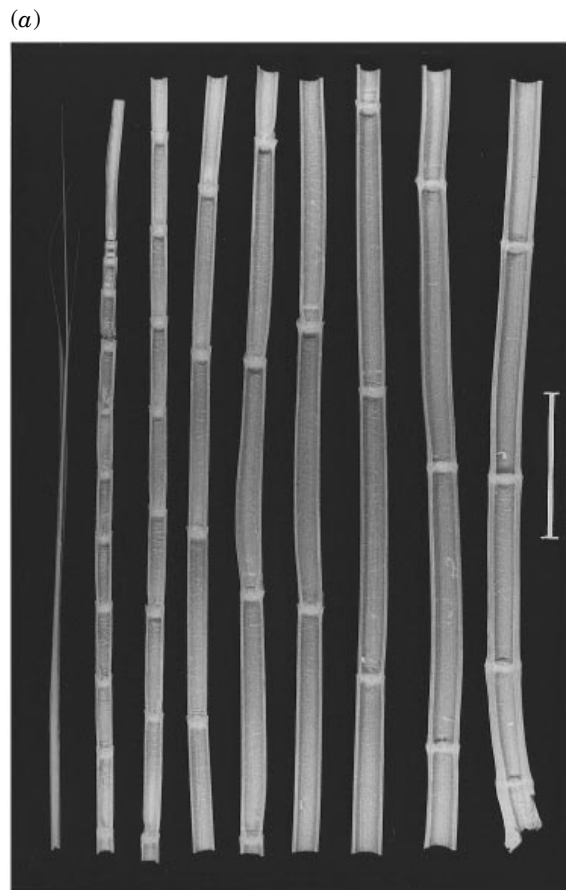


Figure 1. (a) Longitudinal sections of a 5 m long stem of *Arundo donax*. The uppermost part, 63 cm long, is the apical leaf sheath which includes the leaves of the apical, not yet elongated internodes. All other leaves and leaf sheaths are removed. The internodal lengths decrease towards the apex and towards the base of the stem; the wall thickness of the internodes increases basipetally in the basal-most internodes.

Euler Buckling

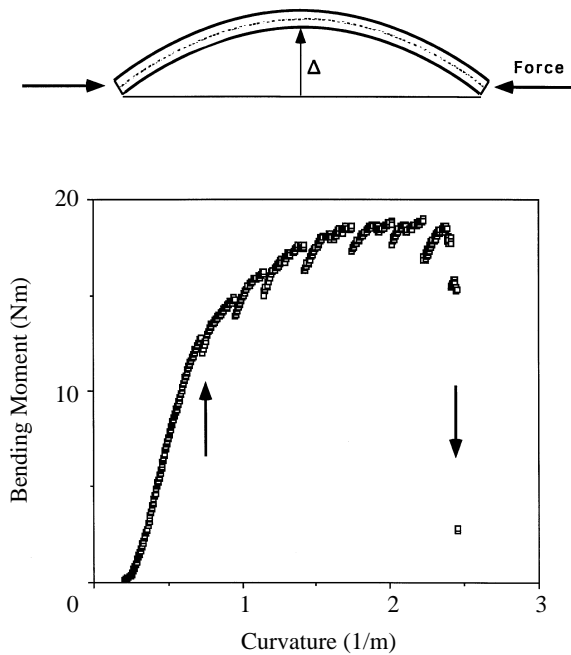


Figure 2. Sketch of Euler buckling. Δ denotes the deflection at the vertex. The diagram shows the relationship between bending moment and curvature for an internode of *Arundo donax* from the upper middle part of the stem. The arrows mark initial failure and final failure. Since bending is carried out under displacement control, a small initial curvature can easily be corrected for by shifting the curve along the horizontal axis.

(c) Structural Young's modulus in the longitudinal direction

Every second internode, plus approximately half of its neighbouring internodes, were subjected to a conventional three-point bending test. The ratio of span to outer diameter was around 15, minimum 10, which for hollow tubes is sufficient to measure true bending. This can be different for solid cylinders of biological material, where the choice of larger span-to-depth ratios is recommended (Spatz *et al.* 1996). No correction was made for the contribution of the nodes, which in *Arundo donax* are stiffer than the internodes but extend only to 0.6 cm as compared to an internodal length of around 20 cm. Additionally longitudinal sections, length *ca.* 5 cm, breadth *ca.* 0.3 cm and depth *ca.* 0.3 cm (= wall thickness of the stem), were prepared from each internode and subjected to three-point bending. The data from this experiment

The scale bar is 10 cm. (b) Cross-section showing a part of the stem wall of an internode from the middle part of the stalk. In our functional analysis we distinguish two tissue types: (i) a hypodermal sterome built up of a ring of sclerenchymatous fibers (sr) with small vascular bundles (svb) including also epidermis (e) with cuticle and the thin layer of photosynthetic tissue (ps); (ii) the thick inner layer of parenchymatous tissue (pt) with significantly lignified cell walls including numerous vascular bundles (vb) with sclerenchymatous bundle sheaths; pith cavity (pc).

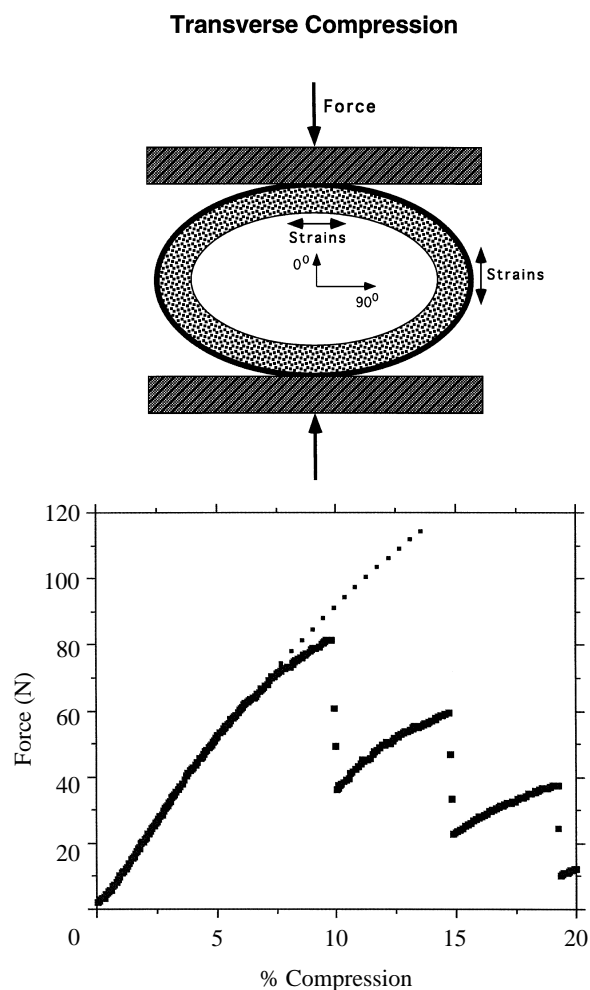


Figure 3. Sketch of the method used to determine Young's moduli in the tangential direction and the relationship between the force applied and the degree of deformation of a segment of an internode of *Arundo donax*. The abrupt decreases of the force mark fracture, first of the parenchyma, then also of the hypodermal sterome. The location of these longitudinal cracks is consistent with the points of maximal tangential tension as indicated above. Experimental data (■); theoretical fit including shear strains (●).

were only used to confirm the results of bending complete internodes.

(d) Euler buckling

Segments of the *Arundo donax* stem of about 50 cm length were subjected to Euler buckling under displacement control (figure 2). Measurement of the force and the deflection Δ allows the calculation of bending moment and curvature at the vertex (Spatz *et al.* 1993) and consequently the determination of the flexural stiffness as well as the critical compression in the longitudinal direction.

(e) Tensile tests

Longitudinal sections of 4–6 cm length and 0.3–0.4 cm width were prepared from each internode. The parenchyma was removed with a scalpel to leave samples of 0.02–0.05 cm depth consisting predominantly of hypodermal sterome. These were subjected

to tensile tests in a device allowing the samples to be submerged in water during the test. Force and displacement transducers were obtained from Burster Präzisionsmeßtechnik, Gernsbach, Germany.

(f) Transverse compression

Several cylindrical segments of 2.0–3.5 cm length were prepared from each internode. In order to assess the gradient of stiffness of the tissues in the radial direction, the parenchyma was scraped out from the inside to various degrees. Displacements and forces to deform a cylinder with the cross-section of a circular ring (figure 3) were measured in the device described above, but samples were not submersed in water. Deforming a thin-walled circular ring to an elliptical ring, where shear does not have to be considered, can be described by elementary mechanics by which the change in the curvature of the ring is proportional to the moment applied. For thick-walled rings, where shear strains have to be taken into account, the situation is considerably more complex and has to be treated numerically (Spatz *et al.* 1995). The structural Young's modulus in the tangential direction was obtained by simulating the data with the help of this numerical description.

(g) Critical tension in the tangential direction

Upon transverse compression the sections fail by splitting at one of the poles of the ellipse, usually first at 0 or 180° (figure 3). The theoretical description of the process of ovalization (Spatz *et al.* 1995) allows the computation of strains at every point along the elliptical ring. Critical tangential strains are defined as the strain, where the first longitudinal split occurs.

(h) Shear modulus

Cylindrical segments of 2.5 cm length were prepared from each internode. Using the device depicted in figure 4, the shear modulus of the parenchyma was determined by torsion of the stiff outer cylinder provided by the hypodermal sterome of *Arundo donax* against a stationary inner cylinder consisting of an aluminum rod glued with Loctite 401 to the parenchyma. The force was applied via sticky tape wound around the outer surface of the specimens. Upon loading with different weights the outer surface moves through an angle β which is obtained from the deflection of a laser light beam by a small mirror glued to the outer surface of the specimen. The shear strain α can be computed from β as described by Spatz *et al.* (1995).

(i) Computation

The numerical description of local buckling is conveniently carried out on a Silicon Graphics workstation. The program is written in Pascal; it is available upon request.

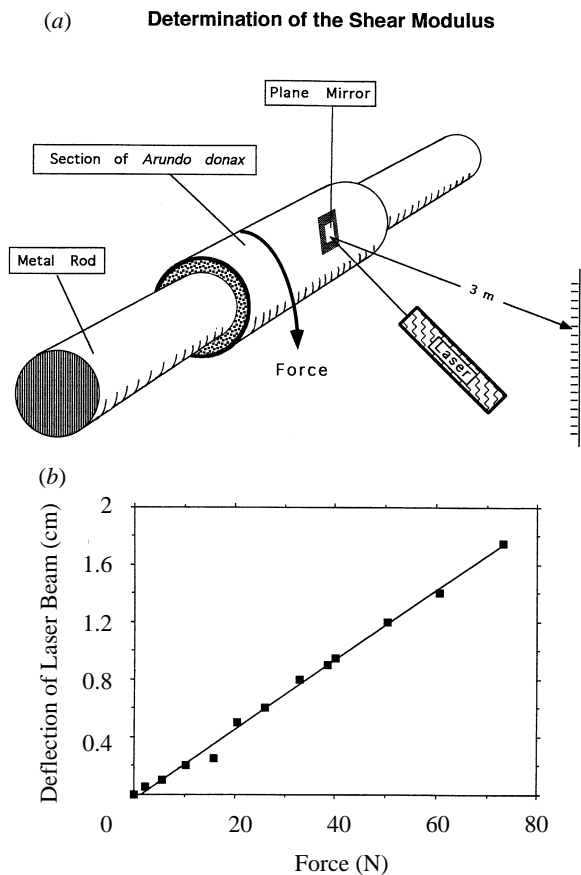


Figure 4. Sketch of the method used to determine the shear modulus for the radial–tangential plane and shear strains as read from the deflection of a laser beam.

3. RESULTS

(a) *Stem anatomy*

The stems of *Arundo donax* are remarkably straight (cf. figure 2, initial curvature). The cross-sections are nearly circular. Measurement of the outer diameter in two orthogonal directions reveals on average a deviation of only 5%. Several stems were subjected to a geometrical analysis. The internodes have a length of typically 22 cm, less in the basal part and much less in the upper 10% of the stem. The outer radius ranges from 1.3 to 0.75 cm, the wall thickness from 0.56 to 0.18 cm. The thickness of the hypodermal sterome was obtained from photographs of thin sections stained with phloroglucinol/hydrochloric acid. It is of the order of 8% of the wall thickness. Figure 5 summarizes these data. In order to relate data from different stems to each other, the values are plotted as a function of the relative height.

(b) *Young's moduli of the hypodermal sterome*

Tensile tests on longitudinally oriented samples, from which the parenchyma was removed, yield Young's moduli in the longitudinal direction of the hypodermal sterome (figure 6). In the lower and the middle part of the stem values around 10 GPa are found, with decreasing values for the uppermost internodes. These values are well in the range of data

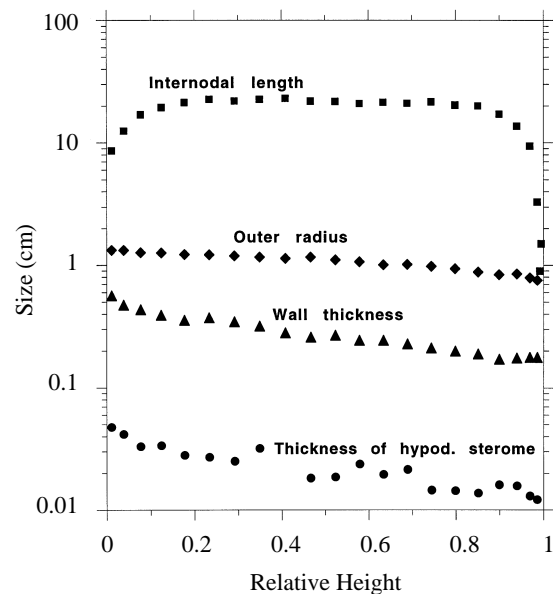


Figure 5. Geometry of a representative *Arundo donax* stem from the Botanical Garden, Freiburg, total height of 3.85 m. The data are plotted as a function of the relative height, where 0 indicates the base of the stem and 1 indicates the most apical tip not including the leaves. Length of internodes (■); outer radius (◆); wall thickness (▲) and thickness of the hypodermal sterome (●).

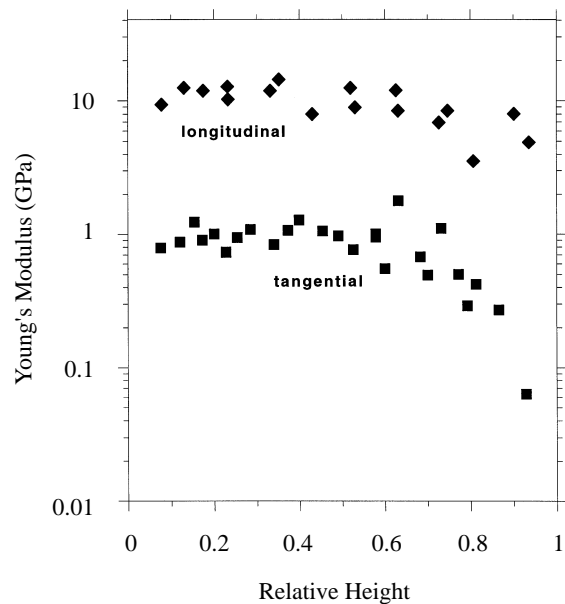


Figure 6. Young's moduli of the hypodermal sterome as function of the relative height of the *Arundo donax* stem: ◆, longitudinal direction; ■, tangential direction.

published for other 'fresh' sclerenchymatous plant fibres which typically range from 5 to 30 GPa (cf. Wainwright *et al.* 1976; Niklas 1992, 1993; Speck *et al.* 1992; Spatz *et al.* 1993; Spatz & Speck 1994) and correspond to the values typically found for 'green' wood ranging from 7 to 18 GPa (cf. Wainwright *et al.* 1976; *Handbook of wood and wood-based materials for engineers, architects, and builders* 1989; Speck *et al.* 1992).

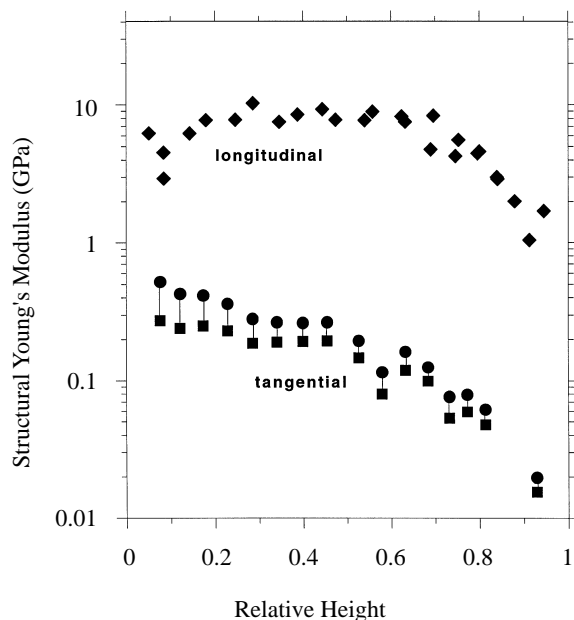


Figure 7. Structural Young's moduli of the parenchyma: longitudinal direction (\blacklozenge); tangential direction neglecting (\blacksquare) and including (\bullet) the contribution of shear strains to the deformation of circular rings.

Young's moduli in the tangential direction are obtained from transverse compression of very thin-walled hollow cylinders (radius around 1 cm and wall thickness below 0.05 cm), prepared by removing all or almost all the parenchyma from segments of each internode (Spatz *et al.* 1995). Young's moduli in the tangential direction average around 1 GPa for the lower and middle part of the stem with a marked decrease for the upper parts of the stem.

(c) *Young's moduli of the parenchyma*

Figure 7 shows corresponding data for the parenchyma. Young's moduli in the longitudinal direction were obtained by subtracting the contribution of the hypodermal sterome from the overall bending stiffness measured in three-point bending. The values average at 9 GPa for the middle of the stem, less in the basal parts and much less in the upper parts. Since the numerous vascular bundles contribute to the stiffness in the longitudinal direction the values should be regarded as structural Young's moduli.

Young's moduli in the tangential direction can be obtained from transverse compression of segments of the stem with intact parenchyma. (Spatz *et al.* 1995). As a first approximation the segment is regarded as composed of a stiff outer ring of hypodermal sterome and a homogeneous inner ring of parenchyma. Young's moduli calculated using the elementary treatment, neglecting shear strains and their correction, using the complete theory including shear strains, are given in figure 7.

(d) *Inhomogeneity of the parenchyma*

The values given for Young's moduli in the tangential direction for the parenchyma are not true

Young's moduli but rather averages weighted with the axial second moment of area and should therefore be referred to as structural Young's moduli. It is noticeable, even without technical means, that the parenchyma is mechanically inhomogeneous with a gradient of stiffness in the radial direction, increasing from the inside to the outside. Figure 8 shows the structural Young's modulus (including the hypodermal sterome) for segments where the parenchyma was removed to various degrees. Each curve derives from segments from one and the same internode. The upper curve is characteristic for an internode near the base with a high degree of lignification throughout, the middle curve is typical for internodes from the major part of the stem and the lower curve is characteristic for an internode near the top with a low degree of lignification and correspondingly a low stiffness. The data can be fitted if it is assumed that the Young's modulus in the tangential direction of the parenchyma in the outermost parts is constant to the point of deflection of the curves and then drops exponentially towards the innermost layer.

(e) *Determination of the shear modulus*

Upon deformation of a circular ring, shear is applied in a radial-tangential plane. Using the device depicted in figure 4, shear strains in this plane can be measured as a function of the force applied. The shear strain is dominated by shear in the innermost layers of the parenchyma, even more so as the degree of lignification decreases from the outside to the inside (cf. figure 8).

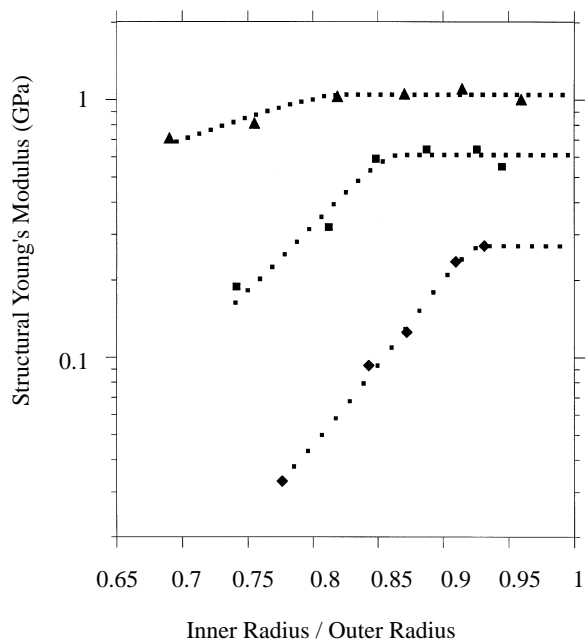


Figure 8. From several segments of an internode the parenchyma was removed to various degrees. The structural Young's modulus in a tangential direction (including contributions from the hypodermal sterome and parts of the parenchyma) is given as a function of the inner radius. Internode near the base (\blacktriangle); internode from the middle of the stem (\blacksquare); internode from the top part (\blacklozenge); fit of the data (\blacksquare).

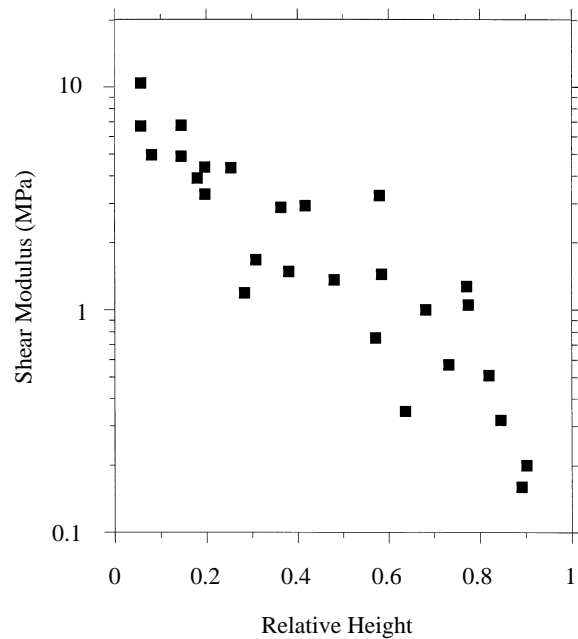


Figure 9. Shear modulus for the radial–tangential plane as a function of the relative height of the *Arundo donax* stem.

The shear modulus, shown in figure 9 as a function of the relative height of the stem, can therefore at least in a first approximation be regarded as the shear modulus G_i for the innermost layer of parenchyma (for a more detailed discussion see Spatz *et al.* 1995).

(f) Estimate of the E/G ratio for the parenchyma

An important mechanical determinant is the ratio of Young's modulus to the shear modulus E/G . In composite materials like wood this is typically much larger than in homogeneous materials (Vincent 1992). At present this ratio can only be obtained for the innermost layer of the parenchyma (Spatz *et al.* 1995) using data like those from figure 8 to calculate the Young's modulus in the tangential direction of the innermost layers of the parenchyma. The E/G value of 11 obtained should be regarded only as an estimate. Whether it is representative for the parenchyma independent of its degree of lignification cannot be answered at present. However, since the contribution of shear to the deformation of segments of the *Arundo donax* stem is not dominant, the corrections of the values for the Young's modulus in the tangential direction (figure 7) seem justified in their order of magnitude.

(g) Critical longitudinal strains

Upon Euler buckling, *Arundo donax* stems will fail partially in compression and ultimately either by local buckling or by longitudinal splitting due to ovalization of the cross-section. A detailed account of these processes has been given previously (Spatz & Speck 1994). Figure 2 shows that failure in Euler buckling is not an all or nothing process. Independent of the relative height of the internode studied, failure proceeds over several discrete audible steps to the final ir-

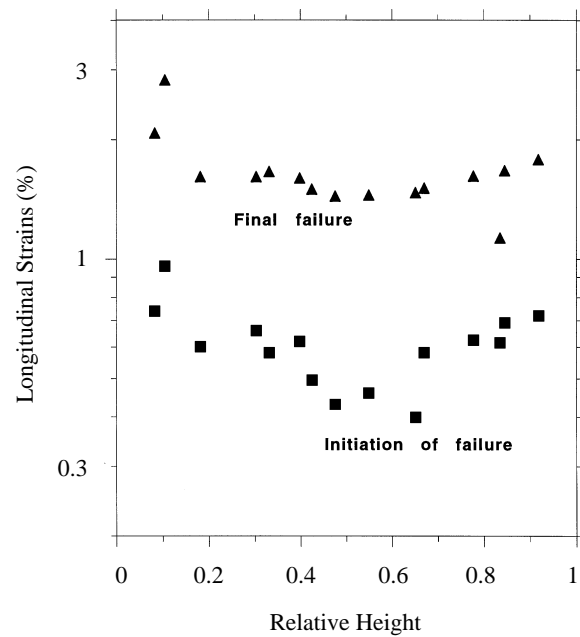


Figure 10. Compressive strains in the longitudinal direction at the points of initiation of failure (■) and final failure (▲). The data sum the strains due to bending and due to compression by the force applied in Euler buckling.

reversible loss of integrity of the structure. Definition of the initial point of failure is somewhat arbitrary. We took the first occurrence of a discontinuity, after which the slope of the moment versus curvature relation had markedly decreased as indication of an initial process weakening the structure.

In Euler buckling, compressive strains result directly from the application of forces in the longitudinal direction and from bending. The latter accounts for the larger part of the strains, even if ovalization of the cross-section is taken into account. Figure 10 shows longitudinal strains at the initiation of failure and strains at the point of final failure as a function of the relative height of the internode tested in Euler buckling.

(h) Critical tangential strains in the parenchyma

Transverse compression leads to failure by longitudinal splitting of the segments tested (figure 11), in most cases initially from inside. The numerical treatment of the ovalization process allows computation of the strains leading to the first longitudinal splitting, where the cross-section still has a near elliptical shape (figure 12).

(i) Critical tangential strains in the hypodermal sterome

For the few cases where segments of *Arundo donax* stems, upon transverse compression, fail first by the splitting of the hypodermal sterome from the outside (i.e. at 90 or 270° of the ellipse), the critical tangential strains for this tissue can be computed. It is found to be remarkably high at around 10%. More data should be obtainable from segments where most or all of the

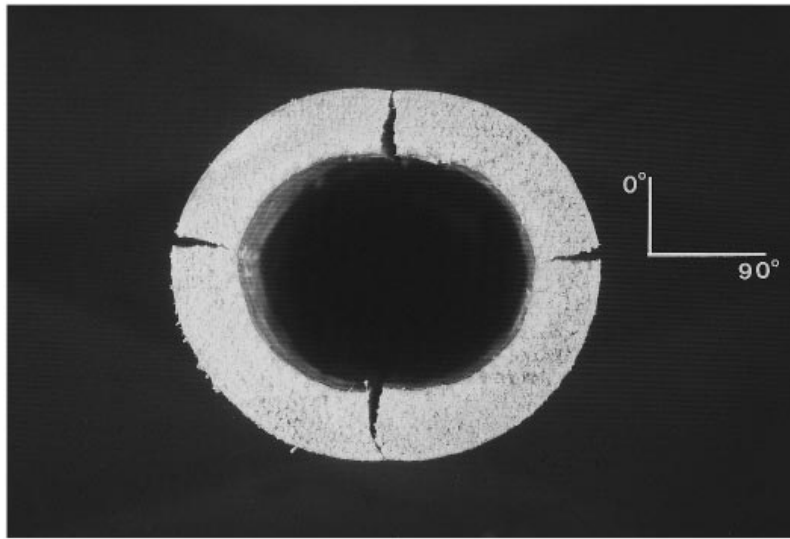


Figure 11. Photograph of a segment of an internode of *Arundo donax* subjected to transverse compression. Longitudinal splitting occurred first in the parenchyma at 0° of the then elliptical ring, subsequently at 180° and upon further compression in the hypodermal stereome at 90 and 270° . Mechanical analysis marks 0 and 180° as the positions of maximal tension on the inside of the ring, and 90 and 270° as those of maximal tension on the outside of the ring.

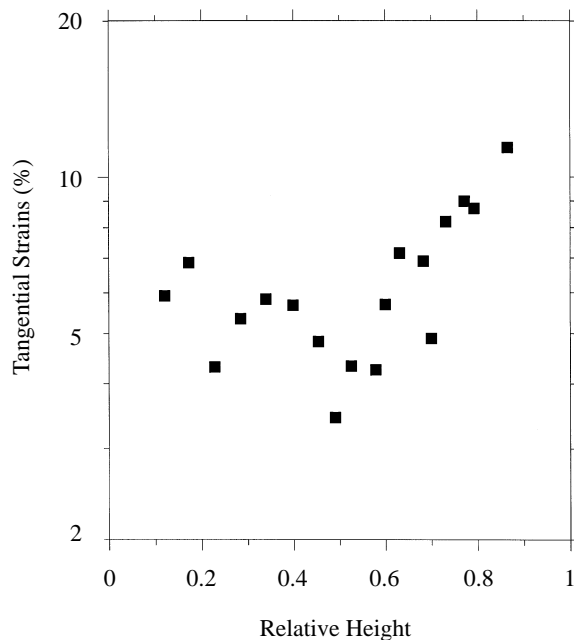


Figure 12. Tangential tensile strains at the point of the first longitudinal splitting in transverse compression.

parenchyma had been removed. Upon transverse compression these segments usually fail by longitudinal splitting through the hypodermal stereome. However, these cracks occur at very large deformations, where the cross-section no longer resembles an ellipse, an assumption underlying our numerical treatment of the ovalization process. Solutions for other geometrical forms of the deformed cross-section remain to be developed.

(j) Does turgor pressure stabilize the structure?

In some hollow plants most notably *Equisetum giganteum* (article in preparation) turgor pressure exerts

a large stabilizing influence against ovalization and local buckling. In order to test this possibility for *Arundo donax*, segments from several internodes along the entire stem were placed in solutions of polyethyleneglycol of different osmolalities (Schopfer 1986) for at least 5 and maximally 15 h and subsequently subjected to transverse compression. A control segment from the same internode was placed in water for the same length of time. Only a small, insignificant and, if at all, positive influence of this treatment can be seen on the structural Young's modulus or on the critical strains in the tangential direction (figure 13).

(k) Maximal bending moments and critical curvature

Figure 14 shows the maximal bending moment reached under conditions of Euler buckling (figure 2) together with the bending moment calculated on the basis of the geometry of the stem tested and the mechanical properties of the tissues. The calculated values are sensitive to the choice of the compressive strains in the longitudinal direction used as limitation for the range of elasticity of the material. We have chosen the strains at the point of initiation of failure (figure 10), as defined in figure 2. For Euler buckling, compressive strains were calculated as result of longitudinal compression and of bending. Provided that the material is more sensitive to compression than to tension, pure bending will tolerate higher bending moments. This is also shown in figure 14. Agreement between the data from direct experiments and those calculated for the equivalent mechanical loading is quite good except for values above 0.8 relative height. It should be pointed out that the Young's moduli, particularly those in the longitudinal direction come from other *Arundo donax* stems to those tested under Euler buckling. Since for the uppermost internodes the degree of lignification and thus the Young's moduli

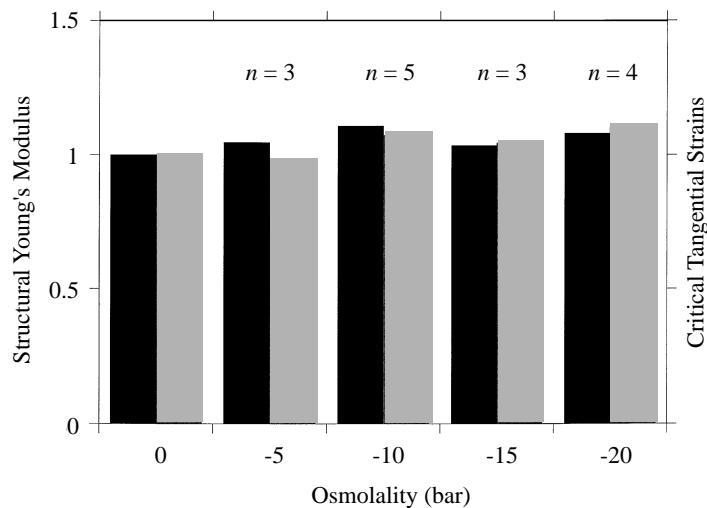


Figure 13. The ratio of the mechanical stability against the transverse compression of the segments of about 3.5 cm length that have been submersed in solutions of polyethyleneglycol of different osmolalities to that of a control segment from the same internode submersed in water. The black bars show Young's modulus and the grey bars show the critical tangential strains.

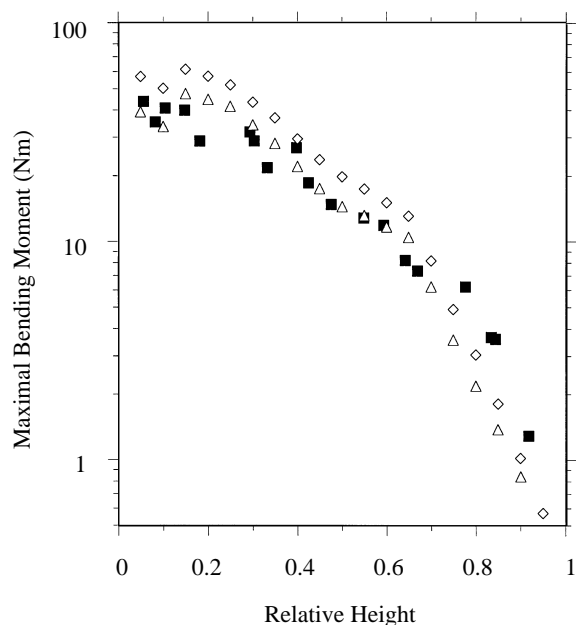


Figure 14. Maximal bending moments determined in Euler buckling (■) as a function of the relative height of an *Arundo donax* stem from a habitat near Montpellier, total height 5.5 m. Calculated values for the maximal bending moments under Euler buckling (Δ) including strains due to longitudinal compressive forces, and for pure bending (\diamond). The values used in these calculations result from second-order polynomial fits to the data or, where this was not feasible, from sliding averages including all values within an interval of ± 0.05 relative height.

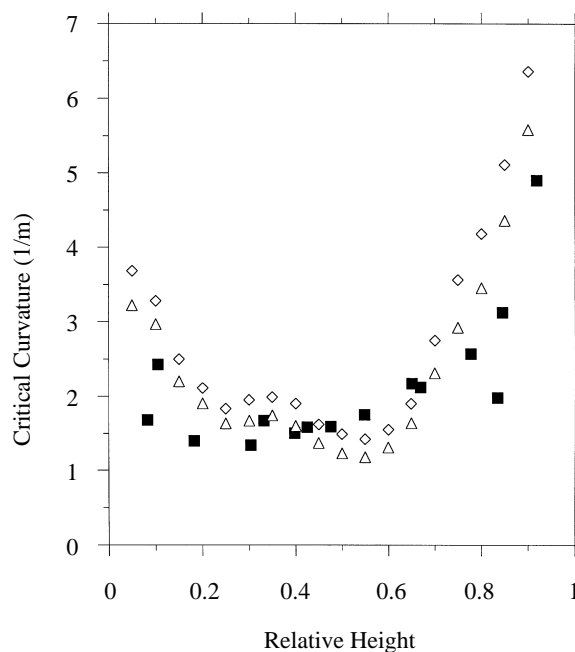


Figure 15. Critical curvature determined in Euler buckling (■) by the same experiments as those for figure 14. Calculated values for the critical curvature under Euler buckling (Δ) including the effects of direct longitudinal forces on the degree of ovalization, and for pure bending (\diamond). The calculations use the values of the tangential strains at the point of the first longitudinal splitting in transverse compression (figure 12) as the critical limit for ovalization and thus as the determinant for final failure.

vary, the differences can be regarded as biological variation.

Since at the point of initiation of failure ovalization is relatively small, the agreement between values from direct experiments and calculation is not a critical test of the theory of local buckling. This is different for the critical curvature (figure 15), where with the exception of the most basal internodes substantial degrees of

ovalization are observed. Except for the geometry the calculated values are based on data, which result from separate experiments, in particular from transverse compression. The computations take into account the stabilizing effect of nodal thickenings (Spatz & Speck 1994). The agreement of calculation and direct experiment for the values of the critical curvature above 0.2 relative height demonstrates that here critical

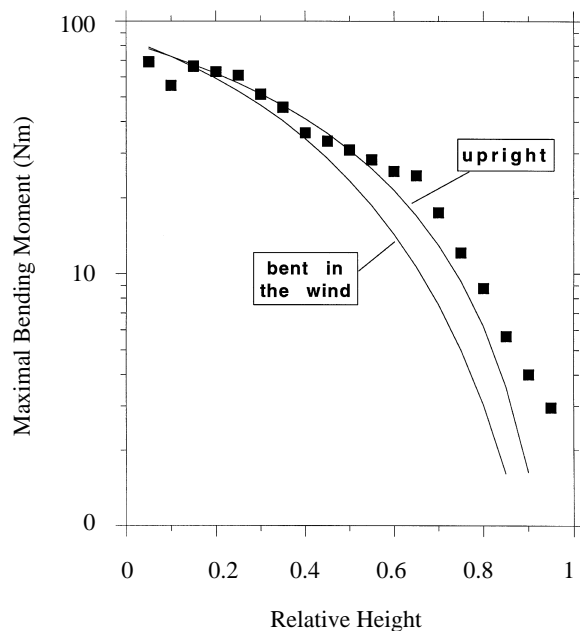


Figure 16. The maximal bending moments calculated for an *Arundo donax* stem from the Botanical Garden, Freiburg, with the geometry given in figure 5, is compared with the bending moments resulting from wind loads on the stem. The effective area is assumed to be $4.2 \times 0.2 \text{ m}^2$. The wind velocity profile is given as $u = u_0 \cdot h^2$, where h is the relative height above ground and u_0 is the wind velocity at the tip of the plant including the uppermost leaf. Two cases are considered, an upright stem and a stem that is bent in the wind into a near hyperbolic shape, such that the tip of the uppermost leaf is only 3 m above ground. A value of $c_w = 1.0$ is used over the entire length irrespective of the degree of leaning in the wind. Values calculated like those for figure 14 but using the geometry given in figure 5 (■); bending moments as a result of wind loads (—); $u_0 = 12.7 \text{ m s}^{-1}$ for the upright stem and $u_0 = 14.5 \text{ m s}^{-1}$ for the stem bent in the wind.

tangential strains, due to ovalization of the cross-section, have led to longitudinal splitting and are thus the primary cause of final failure of the hollow stem. At the most basal internodes and in one case at 0.835 relative height it seems to work the other way round. The material fails primarily in compression and longitudinal cracks are a secondary result of deformation.

(I) Wind forces and mechanical stability

Stability against bending can be set in perspective to the line loads exerted by wind acting on the entire plant including the leaves. Wind loads on plants are notoriously difficult to calculate. The wind profile used takes into account the effects of the canopy (Bussinger 1975; Campbell 1977). Two cases are treated. One case considers an upright stem, the other considers a stem which is bent in the wind such that the curvature at no point exceeds 0.4 m^{-1} , i.e. bending remains below the point of initiation of failure. Figure 16 shows the results of such computations which should only be regarded as a first approximation. Within these limits an *Arundo donax* typical for the location in the Botanical Garden in Freiburg seems to be able to withstand

winds of 13 m s^{-1} measured at a height of 4 m above ground. This corresponds roughly to winds of 18 m s^{-1} measured at a height of 10 m. If allowed to bend in the wind it can tolerate winds of 23 m s^{-1} measured 10 m above ground. Even stronger winds would lead to higher degrees of bending and the partial giving-way of the structure but not necessarily to its destruction.

4. DISCUSSION

Arundo donax is a fast growing plant, yet it possesses a remarkable mechanical stability, independent of turgor pressure. For most of the plant it is the stem that provides resistance to bending moments. However, above a relative height of 0.8 the leaf sheaths provide an effective support for the growing zones and those internodes where the process of lignification has only just started, as witnessed by relatively low Young's moduli (figure 6 and 7).

The stem is composed of two stabilizing tissues, the hypodermal sterome and the parenchyma, which is partially lignified. Both tissues show pronounced anisotropy. In the hypodermal sterome Young's modulus in the longitudinal direction is ten times higher than that in the tangential direction (figure 6). An even larger ratio of the structural Young's moduli in the longitudinal and the tangential direction is found in the parenchyma (figure 7). This is explained by a high degree of lignification but is also due to the reinforcement through heavily sclerenchymatized vascular bundles. It should be noted that the extraordinary stiffness of the parenchyma is the reason why reeds for woodwind instruments can be cut from *Arundo donax*. Indeed, Young's modulus in the longitudinal direction of the parenchyma almost matches that of the hypodermal sterome (figures 6 and 7). Most remarkably, the gradient in radial direction of the Young's modulus in the tangential direction leads to a match of the mechanical properties of the outer layers of the parenchyma with those of the hypodermal sterome as well (figure 8).

As long as integrity of a structure is maintained and sliding does not occur, strains have to be a continuous function in all three dimensions. This can lead to high shear stresses at the borderline between materials with different Young's moduli. *Arundo donax* has 'solved' the problem by establishing a gradient of lignification such that a near perfect match of the mechanical properties between the hypodermal sterome and the outer layers of the parenchyma is accomplished. It is this 'principle of continuity of stresses' that enables the plant to utilize the parenchyma as load-bearing tissue. Along the same line the most basal internodes are characterized by a large wall thickness, while the parenchyma has a relatively low Young's modulus in the longitudinal direction (figure 7). Presumably this allows a smooth transmission of forces to the anchorage system. Provided that the match in mechanical properties is paralleled by a match in the thermal expansion coefficients the design of such a structure could also help to avoid shear separation upon large temperature changes as experienced in the natural habitat of *Arundo donax*.

Failure upon bending is a complex process. Initially strains in the longitudinal direction lead to a series of partial collapses (figure 2). These are presumably due to Euler buckling of groups of vascular bundles and partial destruction of the embedding parenchyma. A test of this presumption will be the subject of a separate report. By sacrificing parts, the structure weakens but is not destroyed. It can even assume a much higher degree of curvature and thus evade wind loads to a considerable degree (Fraser 1962). The limits of this strategy are reached when ovalization of the cross-section leads to tangential strains sufficient to induce longitudinal splitting, which irreversibly destroys the structure.

Arundo donax was originally chosen because all the parameters necessary as input data for the theory of local buckling are accessible in this plant. As seen in figure 14 and particularly figure 15 it served this purpose well. It is of particular importance that the theoretical analysis helps to distinguish primary and secondary causes of failure. Knowing the stem anatomy and a small set of mechanical characteristics of the tissues comprising the stem we are now in a position to predict the mechanical stability of hollow plant stems even from fossil records.

We thank Ms O. Speck, Dr G. Jeronimidis and Dr J. Vincent for helpful discussions and suggestions and U. Eberius for the illustrations.

REFERENCES

- Brazier, L. G. 1927 On the flexure of thin cylindrical shells and other 'thin' sections. *Proc. R. Soc. Lond. A* **116**, 104–114.
- Bussinger, J. A. 1975 Aerodynamics of vegetated surfaces. In *Heat and mass transfer in the biosphere* (ed. D. A. de Vries & N. H. Afgan). New York: Wiley.
- Campbell, G. S. 1977 *An introduction to environmental biophysics*. New York, Heidelberg, Berlin: Springer-Verlag.
- Fraser, A. I. 1962 Wind tunnel studies of the forces acting on the crowns of small trees. *Rep. forest Res.* 178–183. *Handbook of wood and wood-based materials for engineers, architects, and builders* 1989 New York, Washington, Philadelphia, London: Hemisphere Publishing Cooperation.
- Kesel, A. B. & Labisch, S. A. 1996 Schlanke Hochbaukonstruktion gras – Adaptive materialanordnung im Hohlrohrquerschnitt. In *Technische Biologie und Bionik 3* (ed. W. Nachtigall), BIONA-report 10, pp. 133–149. Stuttgart: Fischer.
- Mattheck, C. 1992 *Design in der Natur. Der Baum als Lehrmeister*. Freiburg: Rombach.
- Niklas, K. J. 1992 *Plant biomechanics*. Chicago: University of Chicago Press.
- Niklas, K. J. 1993 Influence of tissue density-specific mechanical properties on the scaling of plant height. *Ann. Bot.* **73**, 173–179.
- Rowe, N. P. & Speck, T. 1996 Biomechanical variation of non-self-supporting plant growth habits: a comparison of herbaceous and large-bodied woody plants. In *L'arbre, biologie et développement, naturalia Monspelienisia, numéro hors série A7* (ed. C. Edelin), Université Montpellier II. (In the press.)
- Schopfer, P. 1986 *Experimentelle Pflanzenphysiologie. Bd. I Einführung in die Methoden*, pp 151. Berlin, Heidelberg, New York, Tokyo: Springer-Verlag.
- Spatz, H.-CH., Speck, T. & Vogelhehner, D. 1990 Contributions to the biomechanics of plants. II. Stability against local buckling in hollow plant stems. *Botanica Acta* **103**, 123–130.
- Spatz, H.-CH., Beismann, H., Emanns, A. & Speck, T. 1995 Mechanical anisotropy and inhomogeneity in the tissues comprising the hollow stem of the giant reed *Arundo donax*. *Biomimetics* **3**, 141–155.
- Spatz, H.-CH., Boomgarden, Ch. & Speck, T. 1993 Contributions to the biomechanics of plants. III. Experimental and theoretical studies of local buckling. *Botanica Acta* **106**, 254–264.
- Spatz, H.-CH., O'Leary, E.-J. & Vincent, J. F. V. 1996 Young's moduli and shear moduli in cortical bone. *Proc. R. Soc. Lond. B* **263**, 287–294.
- Spatz, H.-CH. & Speck, T. 1994 Local buckling and other modes of failure in hollow plant stems. *Biomimetics* **2**, 149–173.
- Speck, T., Schmitt, M., Stahmer, E.-M., Uhl, G., Lange, J. & Parnesar, A. 1992 Mechanische Werte. In *Biologie im Überblick, Lexikon der Biologie, Bd. 10* (ed. M. Schmitt), pp. 244–247. Freiburg: Herder-Verlag.
- Vincent, J. F. V. 1992 Plants. In *Biomechanics, materials, a practical approach* (ed. J. F. V. Vincent), pp. 165–191. Oxford, Tokyo: IRL Press at Oxford University Press.
- von Kármán, Th. 1911 Über die Formänderung dünnwandiger Rohre, insbesondere federnder Ausgleichsrohre. *Z. Ver. deutsch. Ing.* **55**, 1889–1895.
- Wainwright, S. A., Biggs, W. D., Currey, J. D. & Gosline, J. M. 1976 *Mechanical design in organisms*. London: Arnold Press.

Received 3 September 1996; accepted 9 September 1996